3

Experimental and Computational Study of Heat Transfer During Quenching of Metallic Probes

B. Hernández-Morales[1], H.J. Vergara-Hernández[2], G. Solorio-Díaz[3] and G.E. Totten[4]
[1]*Universidad Nacional Autónoma de México,*
[2]*Instituto Tecnológico de Morelia,*
[3]*Universidad Michoacana de San Nicolás de Hidalgo,*
[4]*Texas A&M University,*
[1,2,3]*México*
[4]*USA*

1. Introduction

Heat transfer from hot bodies such as steel, aluminum and other metals is vitally important for a wide range of industries such as chemical, nuclear and manufacturing (including steel hardening) industries. Hardening of steels (so-called martensitic- or bainitic-hardening) requires preheating (austenitizing) of the part to temperatures in the range of 750-1100 °C, from which the steel is quenched (*i.e.*, rapidly cooled) in a defined way to obtain the desired mechanical properties such as hardness and yield strength. Most liquid quenchants used for this process exhibit boiling temperatures between 100 and 300 °C at atmospheric pressure. When parts are quenched in these fluids, wetting of the surface is usually time dependant, which influences the cooling process and the achievable hardness (Liscic *et al.*, 2003).

Heat transfer research related to cooling has been the source of fundamental studies since the early work by Fourier (Fourier, 1820). These early studies were typically performed by hot-wire anemometry (King, 1914; Russell, 1910). One of the first to report the results of fundamental heat transfer studies for the quenching of metals such as steel using cooling curve analysis (time *vs.* temperature curves) was Benedicks who utilized 4-12 mm diameter x 15-50 mm cylindrical carbon steel probes in his now-classic work (Benedicks, 1908). The advantage of using probes larger in diameter than thin platinum wire used for hot-wire anemometry tests is that it is possible to more easily measure thermal gradients through the cross-section upon cooling and to view surface cooling mechanisms. Benedicks work involved cooling hot steel (1000 ^{o}C) in water at 4.5 – 16 ^{o}C and in addition to cooling time from 700 ^{o}C – 100 ^{o}C, effects of the ratio of mass/surface area on cooling time were evaluated.

In 1920, Pilling and Lynch measured the temperature at the center of 6.4 mm dia x 50 mm cylindrical carbon steel probes cooled (quenched) from 830 ^{o}C into various vaporizable liquids (Pilling & Lynch, 1920). From this work, they identified three characteristic cooling mechanisms, so-called: A, B and C-stage cooling which are currently designated as film boiling, nucleate boiling and convective cooling, based on the cooling time-temperature and

cooling rate – temperature profiles. Scott subsequently developed graphical methodology for estimating heat transfer coefficients from the centerline cooling curves of steel probes (Scott, 1934).

At approximately the same time, French reported cooling curve results measured at the surface and center of cylindrical and spherical probes (12.7 – 280 mm dia) quenched into a series of vaporizable liquids from 875 ºC (French, 1930). In addition to studying the effect of agitation, oxidation and surface roughness on cooling velocity, French performed photographic examination of the different cooling mechanisms occurring during the quench processes. These were among the very first pictorial studies illustrating surface wetting differences throughout the quenching process. Similar photographic studies were performed by Sato for examining the effect of facing materials on water quenching processes (Sato, 1933).

Speith and Lange used 10-20 mm cylindrical and spherical copper probes and spherical silver probes to examine quenching processes (Speith & Lange, 1935). The cooling media included tap water, distilled water and rapeseed oil. In addition to cooling curve behavior, they also studied the boundary surface conditions and vapor film formation and breakage on the quenching process using schlieren photography.

Using a 25.4 mm spherical silver probe with a center thermocouple and another exposed at the surface of the ball, T.F. Russell obtained time-temperature cooling curves after quenching in petroleum oil (Russell, 1939). In addition, photographs were taken throughout the quenching process and, like Speith and Lange, showed that that the vapor film which is formed initially on the surface breaks down at a characteristic point. However, Russell did show that the breakage of the vapor film did not occur uniformly on the entire surface. Instead, he observed that the bottom of the probe took longer to reach the characteristic transition temperature than did the sides of the ball indicating non-uniform film formation and rupture over the entire surface of the ball during the quenching process.

Tagaya and Tamura were the first to perform a detailed correlation between surface cooling curves obtained with a 10 mm dia x 300 cylindrical silver probe with a surface thermocouple and movies of the quenching process (cinematographic methods) of the observed cooling mechanisms as they relate to surface wetting processes during quenching (Tagaya & Tamura, 1952). By using a silver probe with a surface thermocouple, they identified four stages of cooling which included the shock-film boiling process that preceeds formation of full-film boiling. Other workers in the field have subsequently used cinematography to study surface heat transfer mechanisms during quenching (Kobasko & Timchenko, 1986; Lainer & Tensi, 1996; Tensi & Lainer, 1999; Narazaki et al., 1999).

Ben David *et al.* have described the rewetting process and the characteristic temperature where this occurs as: "Rewetting of hot surfaces is a process in which a liquid wets a hot solid surface by displacing its own vapor that otherwise prevents contact between the solid and liquid phases. When a liquid contacts a sufficiently hot surface it comes to a boiling point, and a vapor film, which separates the liquid from the surface, is generated. As the surface cools off, the vapor film reaches a point where it can no longer be sustained. At this point, the vapor film collapses and surface liquid contact is reestablished. This phenomenon is called re-wetting or quenching" (Ben David *et al.*, 1999). The temperature at the solid-liquid-vapor contact line is designated as the rewetting temperature or Leidenfrost temperature (Frerichs & Luebben, 2009). Specific knowledge of the rewetting process is especially important because the highest heat transfer coefficient occurs during rewetting.

G. J. Leidenfrost described the wetting process about 250 years ago (Leidenfrost, 1966). Literature describes Leidenfrost temperature-values for water at atmospheric pressure between 150 and 300°C (Yamanouchi, 1968; Duffly & Porthouse, 1973; Kunzel, 1986; Hein, 1980). The Leidenfrost Temperature is influenced by a variety of factors, some of which cannot be quantified precisely even today.

For a nonsteady state cooling process, the surface temperature at all parts of the workpiece is not equal to the Leidenfrost Temperature at a given time. When the vapor blanket (or film boiling) collapses, wetting begins by nucleate boiling due to the influence of lateral heat conduction (relative to the surface) (Ladish, 1980). This is due to the simultaneous presence of various heat transfer conditions during vapor blanket cooling (or film boiling [FB]), nucleate boiling [NB], and convective heat transfer [CONV] with significantly varying heat transfer coefficients α_{FB} (100 to 250 kW m^{-2} K^{-1}); α_{NB} (10 to 20 kW m^{-2} K^{-1}), and α_{CONV} (ca. 700 W m^{-2} K^{-1}). Figure 1 schematically illustrates the different cooling phases on a metal surface during an immersion cooling process with the so-called "wetting front," w, (separating the "film boiling phase" and the "nucleate boiling phase") and the change of the heat transfer coefficients, α, along the surface coordinate, z, (mantle line). In most cases during immersion cooling, the wetting front ascends along the cooling surface with a significant velocity, w, whereas during film cooling the wetting front descends in the fluid direction (Liscic *et al.*, 2003; Stitzelberger-Jacob, 1991).

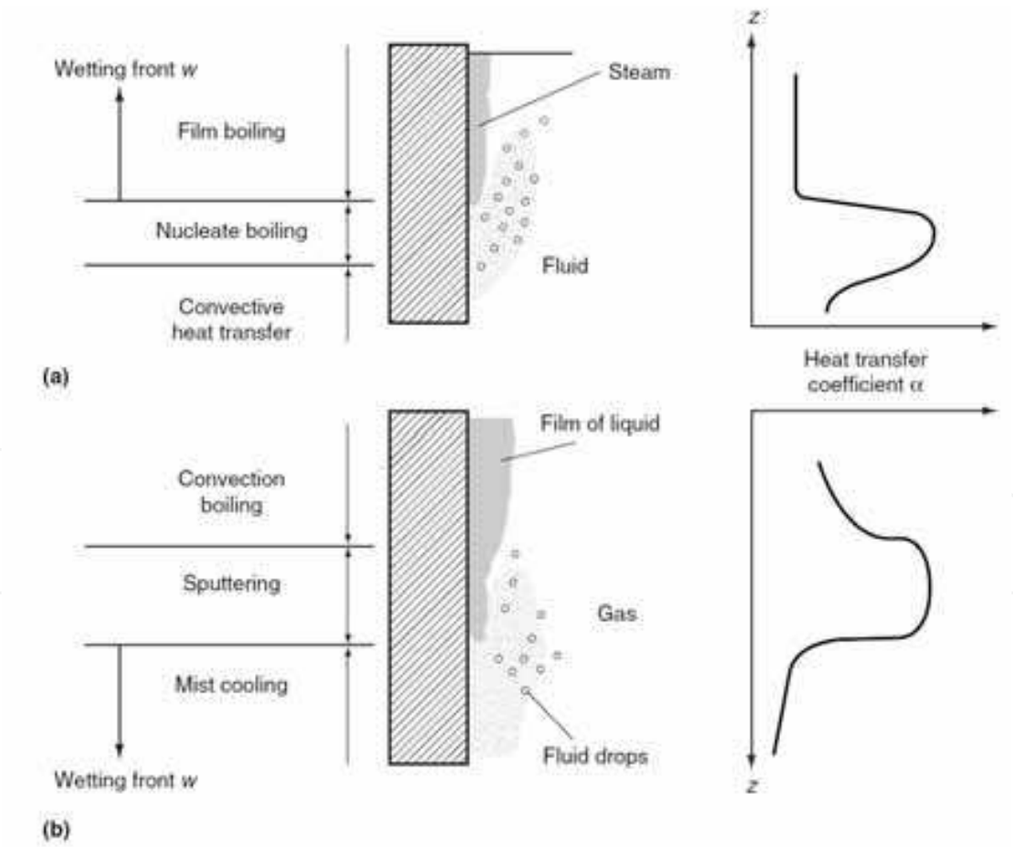

Fig. 1. Wetting behavior and change of heat transfer coefficient (α) along the surface of a metallic probe: (a) immersion coling, (b) film cooling (Liscic et al., 2003; Stitzelberger-Jacob, 1991).

A rewetting process for a heated cylindrical test specimen which was submerged in water is shown in Figure 2 (Tensi & Lainer, 1997; Tensi, 1991; Tensi *et al.*, 1995). Because of the different wetting phases on the metal surface (and the enormous differences of their values of αFB, αNB, and αCONV) the time dependant temperature distribution within the metal specimens will also be influenced by the velocity and geometry of the wetting front (for example, circle or parabolic-like) as well as geometry of the quenched part. Tensi et al. (Tensi et al., 1988) and Canale and Totten (Canale & Totten, 2004) have reported that the degree of non-uniformity of this rewetting process may be sufficiently significant that it will lead to quenching defects such as non-uniform hardening, cracking and increased distortion. Therefore, the understanding and quantification of surface rewetting during quenching by immersion in vaporizable fluids is critically important.

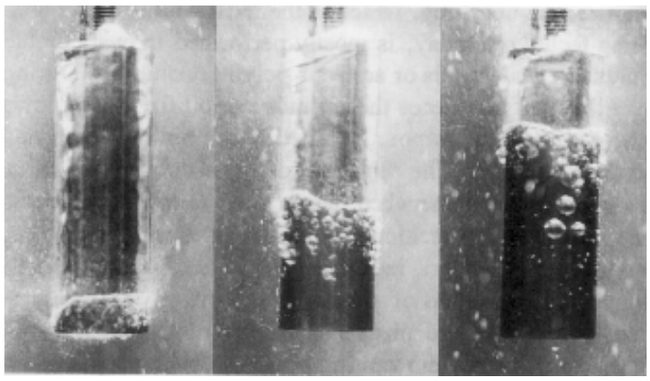

Fig. 2. Cooling process illustrating the transition of the three cooling mechanisms – film boiling (FB), nucleate boiling (NB), convective cooling (CONV) - during immersion cooling of a cylindrical 25 mm dia × 100 mm CrNi-steel test specimen quenched from 850°C into water at 30°C with an agitation rate of 0.3 m/s (Tensi, 1991).

Various methods have been used to quantify the rewetting kinematics of different quenching processes. One of the earlier methods was to place surface, or near surface thermocouples at known positions on a probe surface (Tensi *et al.*, 1995; Narazaki *et al.*, 1999). Although any probe shape could be employed, most typically a cylindrical probe is used. However, it is important to note that when cylindrical probes are used, probe shape of the bottom surface is important (Tensi & Totten, 1996). It has been shown by various workers that perfectly flat surfaces are often not preferred because of their potential impact on the stability of the film-boiling process and subsequent transition to nucleate boiling; the so-called edge effect (Narazaki *et al.*, 1996). Recently, a preferred probe design has been proposed for use in studying rewetting kinematics of immersion quenching processes (Vergara-Hernández & Hernández-Morales, 2009).

Tensi *et al.* have used electrical conductance measurements to quantify wetting kinematics for classification of the overall rewetting processes that may be encountered and for subsequent modeling work (Tensi *et al.*, 1988). This is based on the fact that the electrical conductance increases significantly as the vapor blanket formed during film boiling ruptures, which is followed by the nucleate boiling process where there is fluid contact at the metal-quenchant interface. The electrical conductance increases as the coverage of the surface with boiling quenchant increases (Totten & Tensi, 2002).

Tkachuk *et al.* have shown the importance of surface wetting properties of both the basestocks used to formulate oil quenchants and the effects of a wide range of different additives on surface wetting, especially as it relates to cooling rates (Tkachuk *et al.*, 1989; Tkachuk *et al.*, 1986). Not unexpectedly, as the wetting properties improve, the heat extraction capability increases resulting in higher cooling rates. However, these measurements were limited to room temperature and they did not describe the rewetting process during quenching using these fluid formulations. More recent work by Jagannath and Prabhu has however addressed many of these shortcomings by utilizing dynamic measurements on the quenching surface (Jagannath & Prabhu, 2009). While they do provide a dynamic measure of overall wetability, such measurements do not provide any quantification of the movement of the wetting front during the immersion quench.

The method of choice to study surface rewetting process involves quantitative cinematography. Various workers have discussed experimental approaches to examining surface rewetting using different probe designs and experimental processes to study immersion quenching in vaporizable fluids (Lainer & Tensi, 1996; Tensi & Lainer, 1999; Hernández-Morales et al., 2009; Lübben et al., 2009; Frerichs & Lübben, 2009). These measurements have been invaluable in providing more realistic assessments in the modeling of heat flux, thermal gradients and residual stresses during quenching such as the work reported by Loshkaroev *et al.* (Loshkaroev *et al.*, 1994).

Given the importance of carefully monitoring the advance of the wetting front and deriving quantitative information about heat extraction during forced convective quenching, in this chapter, we describe detailed computational and experimental work to asses the usability of probes of different geometries. Also, results of wetting front kinematics and heat extraction obtained with a conical-end cylindrical probe are presented.

2. Experimental work

The experimental apparatus is shown in Figure 3. The water in the main container is drawn with a ¼ HP pump and flows through a 90° elbow followed by a vertical plexiglass tube (44 mm I.D.). The water flowrate is set with a rotameter which is placed before the 90° elbow. After impacting the probe, the water is discharged in a secondary container. The desired water temperature is achieved with electrical heaters placed within the main container; the water temperature control was manual.

From PIV (Particle Image Velocimetry) measurements conducted at several distances from the elbow it was found that the velocity profile was not fully developed until a position of 1.50 m along the vertical section of the plexiglass tube (Vergara-Hernández & Hernández-Morales, 2009). Thus, the probe tip was always located at 1.70 m from the elbow. The probe was heated in an electric furnace (in stagnant air) up to a temperature of 915 °C such that the temperature at the start of the quench was close to 900 °C in all experiments. To ensure a quick and controlled descent of the probe into the quench bath, the probe was attached to a steel lance which in turns was fitted to a moving spreader.

Three probe geometries were considered: 1) flat-end cylinder, 2) hemispherical-end cylinder and 3) conical-end cylinder. The probes were machined from AISI 304 stainless steel stock bar and instrumented with 1/16", Inconel-sheathed, type K (see Figure 4). The thermocouples were press-fitted into position. To keep water to enter into the space between the thermocouple and the bore wall, the top surface of the probe was covered with high temperature cement (Omega, model Omega 600).

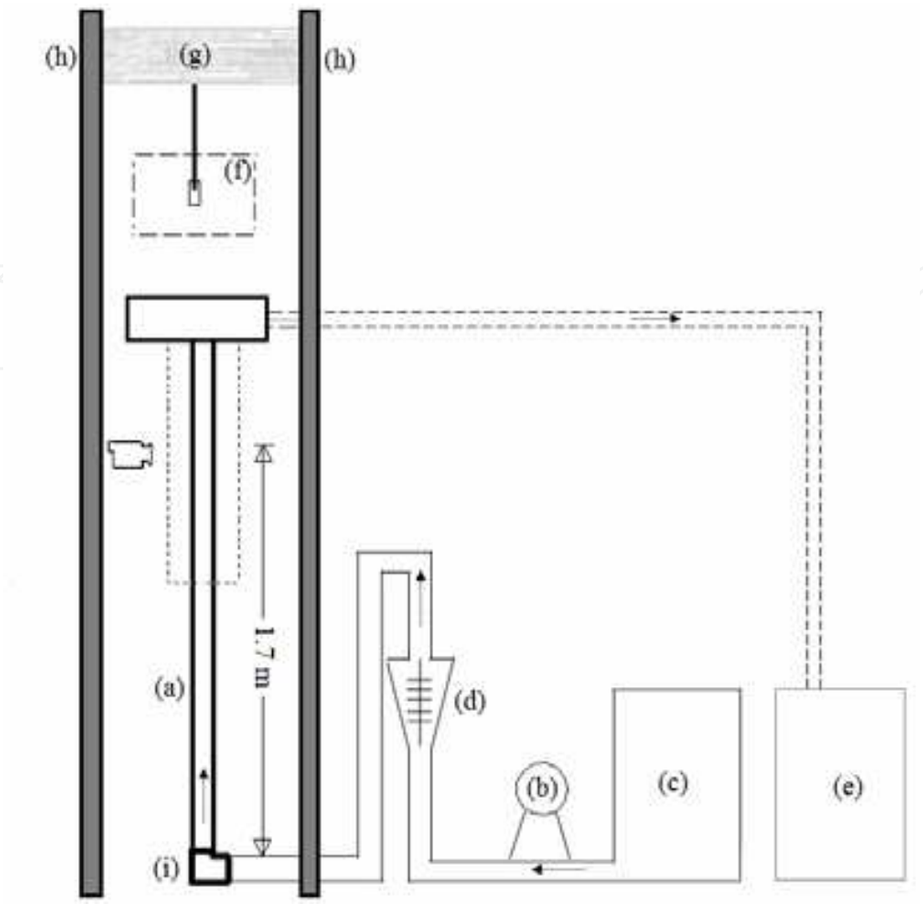

Fig. 3. Schematic representation of the experimental device: (a) plexiglass tube, (b) pump, (c) primary water container, (d) rotameter, (e) secondary water container, (f) electrical furnace, (g) moving spreader, (h) supports, (i) 90° elbow.

The events occurring at the probe surface during the quench were recorded with a high-velocity camera (Photron, model FASTCAM-PCI R2). The camera was placed in front of the tube at the probe quenching position, approximately 50 cm from the external wall of the tube; the videos were recorded at 125 fps with a resolution of 512 X 480 pixels. To avoid image distortion, a glass container (8 cm × 8 cm × 60 cm, with a 46 mm dia. hole at the center of its base) filled with water was placed surrounding the tube, vertically-centered at the probe quench position. To record the thermal response, the thermocouples were connected to a computer-controlled data acquisition system (IOTECH, model TempScan1000); the software package ChartView 1.02 was used to control the data acquisition operation. A data acquisition frequency of 10 Hz was used for all experiments.

In addition to the quenching experiments, physical modeling (cold) tests were conducted to visualize the flow of water in the neighborhood of the probe. The experiments were carried out with the whole system at room temperature; cellophane ribbons were attached to the probe base (or the probe tip, in the case of the hemispherical-end and the conical-end cylindrical probes) to show the flow streamlines. The cold experiments were conducted for each one of the three water velocities of interest.

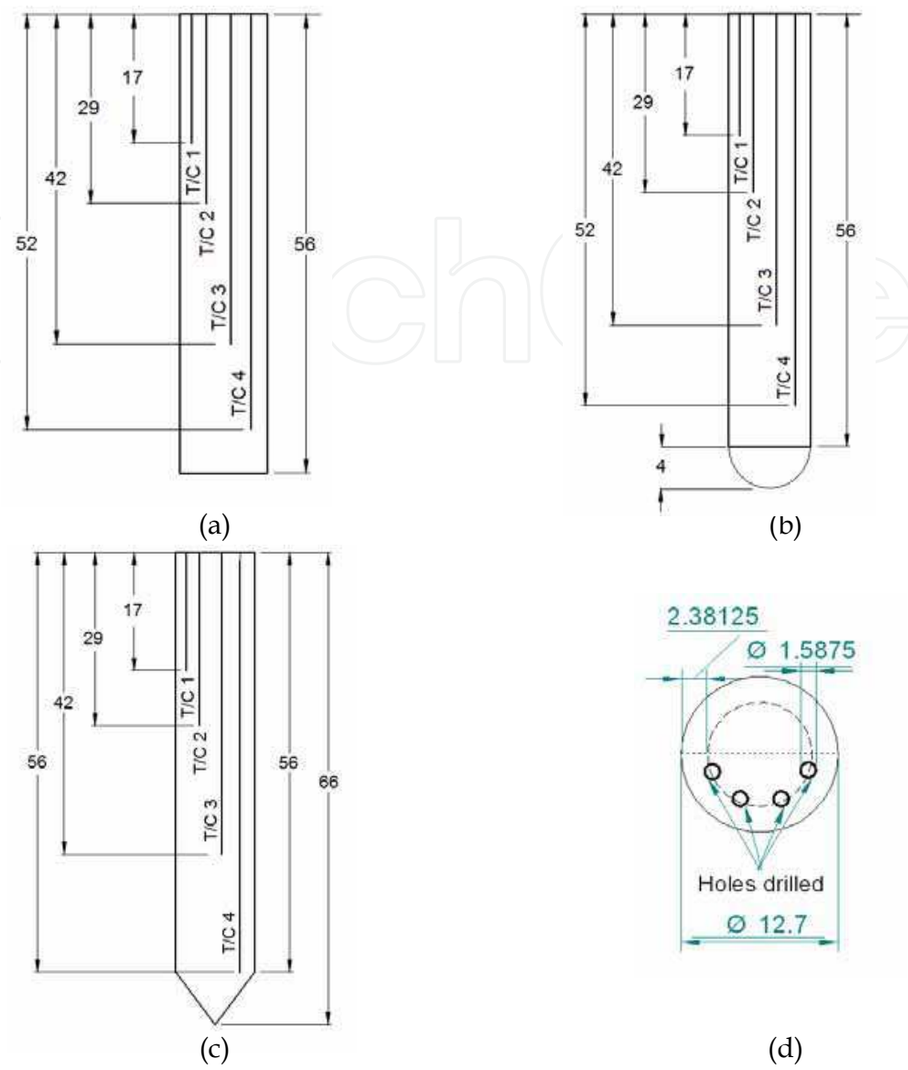

Fig. 4. Test probes: (a) conical-end cylindrical probe (lateral view); (b) hemispherical-end cylindrical probe (lateral view); (c) flat-end cylindrical probe (lateral view); (d) top view. All dimensions are in millimeters.

3. Mathematical model

In previous reports (Vergara-Hernández & Hernández-Morales, 2009; Vergara-Hernández *et al.*, 2010; Hernández-Morales *et al.*, 2011), mathematical models of fluid flow were used to explore the effect of the hydrodynamic characteristics within the water flowing past the probes on the heat extraction for the flat-end and the conical-end cylindrical probes. In this work, those computations are extended to include the hemispherical-end cylindrical probe in order to provide with a clear picture of the effect of the fluid-solid interactions and their impact on the heat extraction.

Assuming that there is no angular component of the velocity within the plexiglass tube, the domain considered in the mathematical model was a 2D (r-z) axis-symmetric plane (see

Figure 5 (a)) where a Newtonian fluid is flowing under unsteady-state conditions; the whole system is treated as isothermal. To optimize computer resources, only half of the plane is simulated.The boundary conditions are indicated in Figure 5 (b). Similar computational domains and set of boundary conditions were used for the simulations corresponding to the hemispherical-end and the conical-end cylindrical probes.

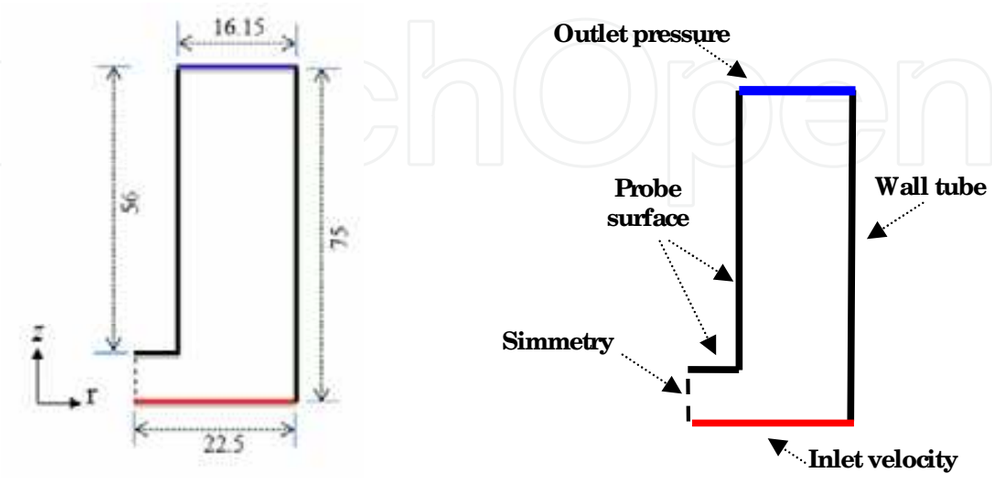

(a) (b)

Fig. 5. (a) Computational domain (dimensions in mm) and (b) boundary conditions for the simulations corresponding to the flat-end cylindrical probe.

The objective of the mathematical model was to relate the hydrodynamic conditions to the characteristics of the vapor film and the re-wetting process by computing the evolution of: 1) the streamlines and 2) the velocity field within the fluid. The simulations were carried out for a system at room temperature and an incompressible fluid. Therefore, the governing equations (continuity and momentum conservation) may be written as:

$$\nabla \cdot \bar{v} = 0 \tag{1}$$

$$\rho\left[\frac{D\bar{v}}{Dt}\right] = -\nabla\bar{p} - \left[\nabla \cdot \bar{\tau}\right] - \left[\nabla \cdot \overline{\tau_R}\right] + \rho\vec{g} \tag{2}$$

Where ρ is the fluid density, v is the fluid velocity vector, p is the dynamic pressure, τ is the stress tensor related to viscous flow τ_R is the Reynolds stress tensor and $\vec{g}$ is the acceleration vector due to the gravitational force. The overbars indicate time-averaged values. The $k-\varepsilon$ turbulence model (Launder and Spalding, 1974) was used to describe the turbulent characteristics of the flow:

$$k = \frac{3}{2}(u_{avg}I)^2 \tag{3}$$

$$I = 0.16(\mathrm{Re}_{D_H})^{-1/8} \tag{4}$$

$$\varepsilon = C_{\mu}^{3/4} \frac{k^{3/2}}{\mathrm{l}} \tag{5}$$

$$\mathrm{l} = 0.07\, L \tag{6}$$

where k and ε are the kinetic energy turbulence and its dissipation, respectively, I is the turbulent intensity, u_{avg} is the average fluid velocity, Re_{D_H} is the Reynolds number based on the hydraulic diameter, l is the turbulent scale length, C_{μ} is a constant (0.09), and L is the duct diameter.

Using information obtained with previously reported PIV measurements (Vergara-Hernández & Hernández-Morales, 2009), the following velocity profile at the bottom boundary of the computational domain (refer to Figure 5 (a)) was applied:

$$u(r) = \left[\frac{(0.2389\text{E-}06+|\mathrm{r}|)}{(0.6791\text{E-}03+1.007\cdot|\mathrm{r}|)} + 7.131\cdot|\mathrm{r}| \right] u_{avg} \qquad -R < r < R \tag{7}$$

Where $u(r)$ is the velocity profile at the inlet of the computational domain, r is the radial position measured from the symmetry plane and R is the tube radius.

The governing equations and related boundary conditions are highly non-linear which forces a numerical solution. The commercial CFD (Computational Fluid Dynamics) code Fluent (Fluent, 2011), which is based on the Finite Volume Method (Versteeg & Malalasekera, 1995), was used. The computational domain was discretized as shown in Figure 6; a total of 42,000 cells (control volumes) were used.

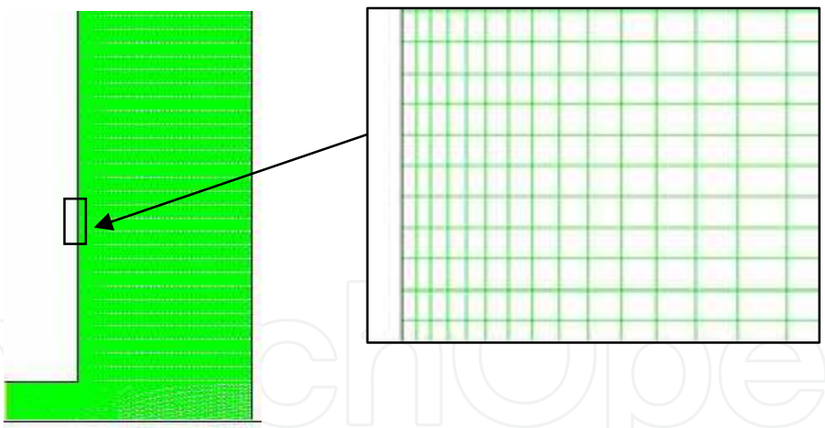

Fig. 6. Mesh used to discretize the computational domain. The image on the right corresponds to a detail showing the mesh near the probe surface.

4. Results and discussion

4.1 Thermal response

The simultaneous occurrence of the three modes of heat extraction and the presence of the wetting front (the boundary between film and nucleate boiling) are evident in Figure 7, which corresponds to a quench in water at 60 °C, flowing at 0.2 m/s. From this image it is clear that the transition from one mode to another is not sharp: on the one hand, the bubble

density in the nucleate boiling region is not constant and, on the other, the probe surface above the wetting front shows areas with different tonalities which implies a surface thermal gradient along the probe length.

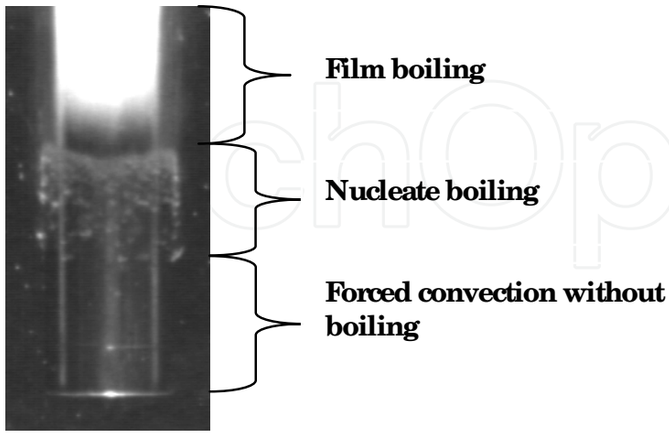

Fig. 7. Heat transfer modes during quenching of a flat-end cylindrical probe quenched from 900 °C in water at 60 °C, flowing at 0.2 m/s. The wetting front occurs at the boundary between the film and nucleate boiling regions.

The thermal response measured at the position of T/C 3 during quenching of a flat-end cylindrical probe from 900 °C in water at 60 °C, flowing at 0.2 m/s and images extracted from the video-recording taken during that experiment are shown in Figures 8 (a) and (b), respectively. Initially, the thermal response follows a horizontal line indicating that the probe is still within the furnace; then a slight drop in temperature, starting at 4.1 s (point "1"), may be seen as the furnace is opened and the probe is transferred to the quench bath. The quench starts at 11.07 s (point "2"), immediately producing a vapor blanket that lasts for 11.8 s and resulting in a temperature decrease that occurs at a constant rate. The local collapse of the vapor blanket at the probe base originates the wetting front, which moves upward. The wetting front is characterized by a high heat extraction associated with the nucleation and growth of the bubbles and reaches the vertical position of T/C 3 at 20 s; then, the local surface temperature drops significantly until it cannot sustain the phase change any longer, giving way to pure forced convection. This behavior is similar to that reported earlier (Stich *et al.*, 1996).

From the measured thermal response shown in Figure 8, the corresponding cooling rate history was obtained by numerical differentiation using a first order polynomial approximation (Carnahan *et al.*, 1969) and is plotted in Figure 9. In accordance with the slope changes observed in Figure 8 (a), there are changes in cooling rate at times corresponding to transferring of the probe from the furnace (Point "1") and immersing it in the quench medium (Point "2"). Once the probe is immersed in the quench medium the cooling rate increase until a steady value of - 23 °C/s is reached, which indicates the presence of the vapor blanket. The maximum cooling rate (- 184 °C/s) occurs at approximately 24.8 s.

Following the same procedure, the cooling rate histories for an experiment conducted with water at 60 °C, flowing at 0.6 m/s, were estimated and are shown in Figure 10.

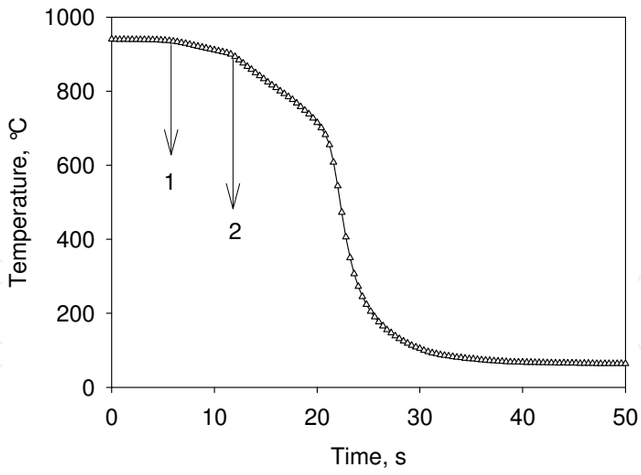

(a)

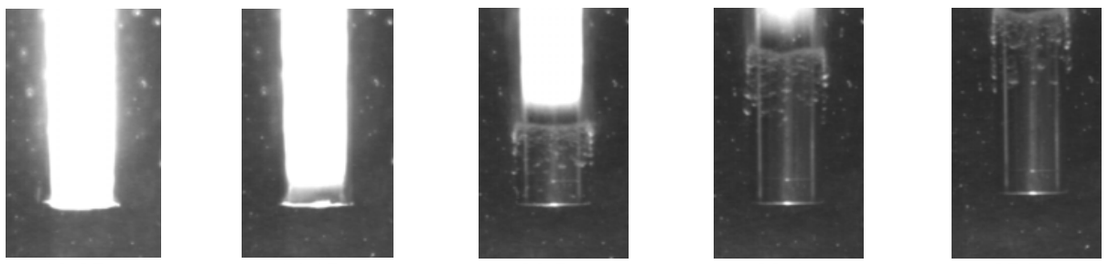

(b)

Fig. 8. (a) Thermal response at the position of T/C 3 measured during quenching of a flat-end cylindrical probe quenched from 900 °C in water at 60 °C, flowing at 0.2 m/s; b) images taken from the video-recording.

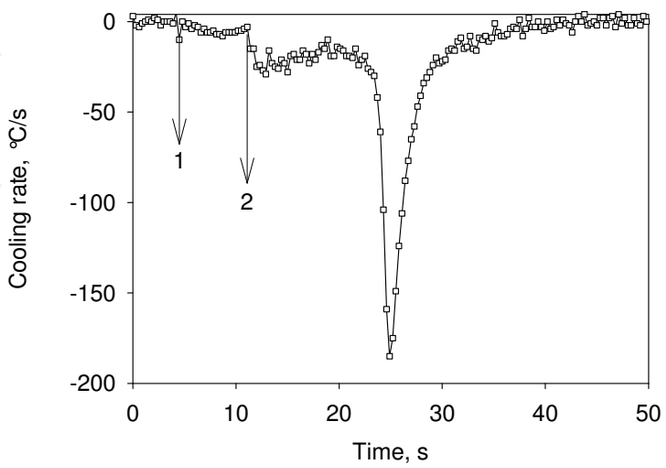

Fig. 9. Cooling rate history at the position of T/C 3 during quenching of a flat-end cylindrical probe in water at 60 °C flowing at 0.2 m/s.

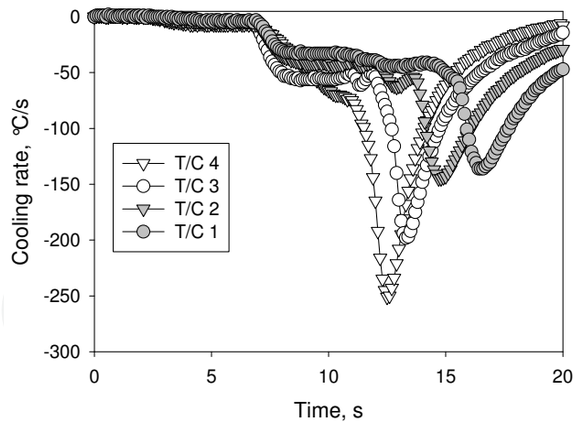

Fig. 10. Cooling rate histories during quenching of a flat-end cylindrical probe from 900 °C in water at 60 °C, flowing at 0.6 m/s.

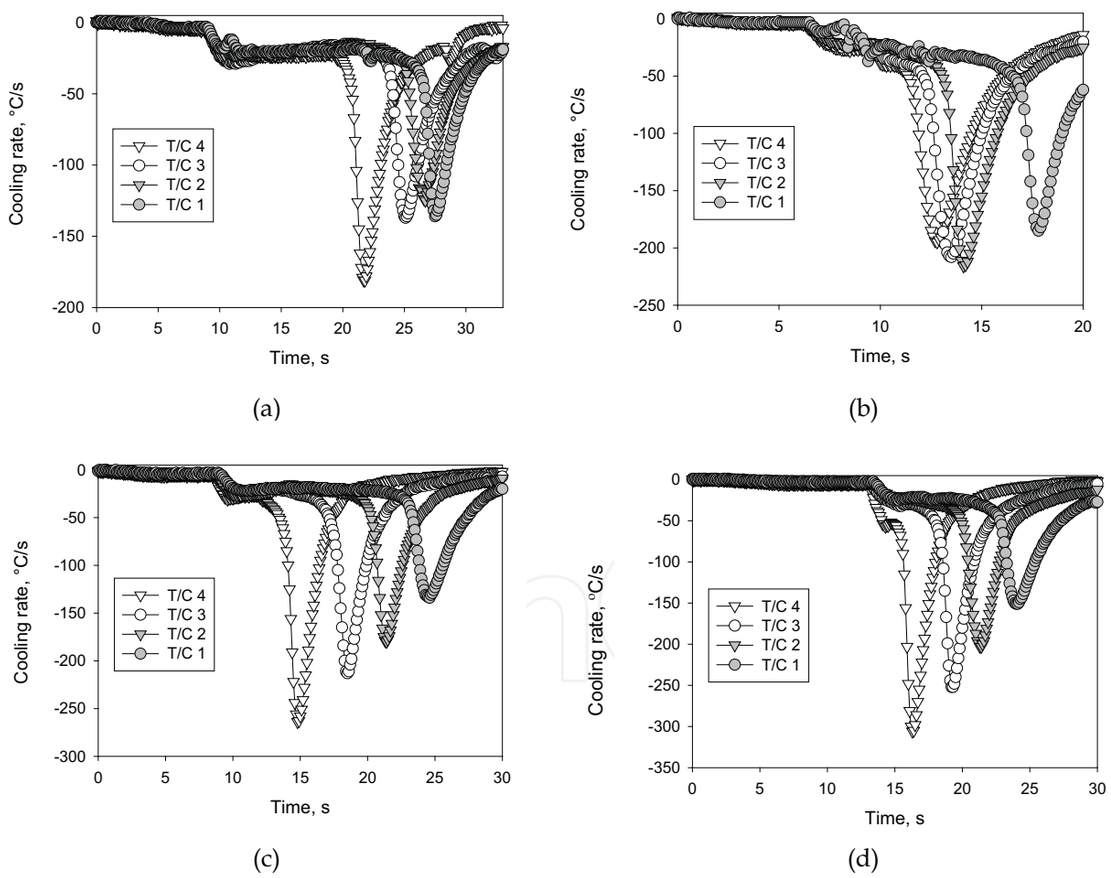

Fig. 11. Cooling rate history during quenching from 900 °C in water at 60 °C for: a) hemispherical-end cylindrical probe in water flowing at 0.2 m/s; b) hemispherical-end cylindrical probe in water flowing at 0.6 m/s; c) conical-end cylindrical probe in water flowing at 0.2 m/s and d) conical-end cylindrical probe in water flowing at 0.6 m/s.

Characteristic parameters of the curves such as the cooling rate during the vapor blanket stage and the maximum cooling rate both increase with respect to the corresponding values observed in Figure 9, as a result of the higher water velocity; for the thermocouple closest to the probe base (T/C 4) there is no evidence of formation of a stable film blanket. Furthermore, during the vapor blanket stage different cooling rates are observed at each thermocouple location and fluctuations around a mean value were detected. These latter observations imply that the vapor blanket is not uniform along the probe length for this value of water velocity.

Figure 11 shows the cooling rate histories when hemispherical-end and conical-end cylindrical probes were quenched in water at 60 °C, at two water velocities: 0.2 and 0.6 m/s. As can be seen in the figures, the cooling rate histories produced with the hemispherical-end probe show less oscillations than the corresponding curves for the flat-end probe (refer to Figure 10) but the time interval between each consecutive pair of maximum values of the cooling rate are not constant, which suggests that the wetting front velocity is not constant along the probe surface. In sharp contrast with the results obtained with the two other geometries, the cooling rate history curves corresponding to the conical-end cylindrical probe are very similar among themselves, for a given water velocity, which indicates that the very same phenomena are occurring at the probe surface. It could be inferred that the wetting front would advance at a constant velocity when this type of probe is used.

4.2 Computational fluid dynamics

From the previous section, it is clear that the probe geometry does have a significant effect on heat extraction during the quench. Assuming that this effect is strongly related to the hydrodynamics of the quench medium flowing past the probe, calculations of hydrodynamic-related fields for the three probe geometries studied were carried out. As a first approximation, the simulations were conducted for both the probe and the water at room temperature, *i.e.*, considering an isothermal system.

The first quantities computed with the model were the streamlines around the probes; these maps could be directly compared to the images obtained during the physical modeling tests, to validate the mathematical model. The results, for the three probe geometries studied and a free-stream water velocity of 0.6 m/s, are shown in Figure 12. In Figure 12 (a) the boundary layer separation is noticeable. This effect does not occur for the hemispherical-end cylindrical probe or the conical-end cylindrical probe.

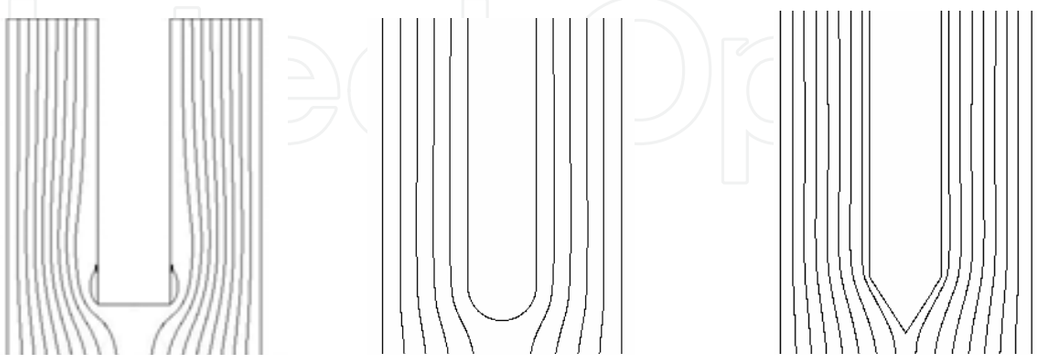

(a) (b) (c)

Fig. 12. Computed streamlines, after 2 s of simulation, for water flowing at 0.6 m/s: (a) flat-end cylindrical probe, (b) hemispherical-end cylindrical probe, and (c) conical-end cylindrical probe.

To produce data necessary to validate the CFD model, cold experiments were run with cellophane ribbons attached to the probe base and the system running at room temperature. From the video-recordings taken during experiments corresponding to the conditions of Figure 12, the three images shown in Figure 13 were extracted. Comparing Figures 12 and 13 it is evident that the computed streamlines compare favorably with the experimental ones; thus, the mathematical model may be considered as validated and may be used for further analysis.

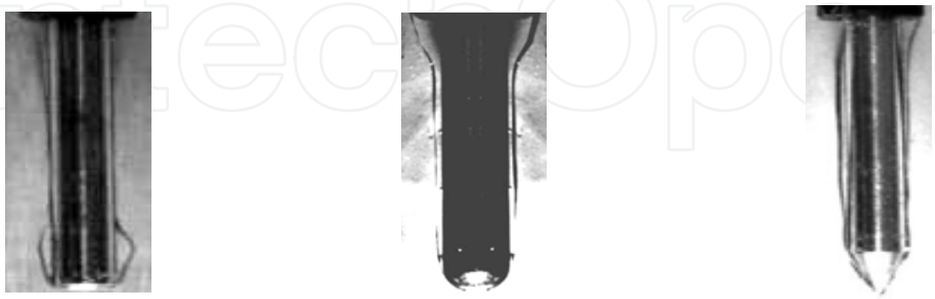

(a) (b) (c)

Fig. 13. Observed streamlines in the neighborhood of (a) flat-end cylindrical probe, (b) hemispherical-end cylindrical probe, and (c) conical-end cylindrical probe, for water flowing at 0.6 m/s.

The computed velocity field (m/s) in the neighborhood of a flat-end cylindrical probe, for two water velocities, is shown in Figure 14. The vertex of the probe produces a significant velocity "jump" even for the lower water velocity; for a water velocity of 0.6 m/s it is evident that backflow occurs, which is responsible of the streamline observed in Figure 13 (a). Figure 15 shows the velocity field (m/s) computed with the CFD model for the hemispherical-end cylindrical probe. At the position of 90° the fluid is nearly stagnant while a noticeable velocity gradient was computed near the 0° position, where siginificant areas with values of nearly 0.33 and 1 m/s were obtained for average free-stream velocities of 0.2 and 0.6 m/s, respectively. The computed velocity field (m/s) for water at room temperature flowing in the neighborhood of the conical-end cylindrical probe at two average free-stream velocities (0.2 m/s y 0.6 m/s) is shown in Figure 16. In contrast with Figure 15, there is a much smaller area where high velocities do exist.

Images of the events occurring at the probe surface during the vapor blanket stage for the three geometries studied are shown in Figure 17. In all cases the quench medium was water at 60°C, flowing at 0.6 m/s. The vapor blanket produced when the flat-end cylindrical probe was used is markedly non-uniform; in particular, it is wider near the probe end, showing an abrupt change afterwards. The image corresponding to the hemispherical-end cylindrical probe shows a much more uniform vapor blanket; nonetheless, a couple of "cold" spots were observed (see the arrows in the figure). On the other hand, using the conical-end cylindrical probe resulted in a very uniform vapor blanket. These different behaviors may be correlated with the velocity fields shown in Figures 14 (b), 15 (b) and 16 (b): as the velocity gradient at the probe surface increases, the probability of the occurrence of a non-uniform vapor blanket also increases. Also, recall that the simulations showed the occurrence of backflow for the flat-end cylindrical probe, over an area which is similar to the area where a thicker vapor blanket was observed.

Finally, in Figure 17 (c) it is observed that the vapor blanket has already initiated its collapse, *i.e.*, re-wetting has started. This effect is due to the higher heat extraction rate promoted by the probe tip.

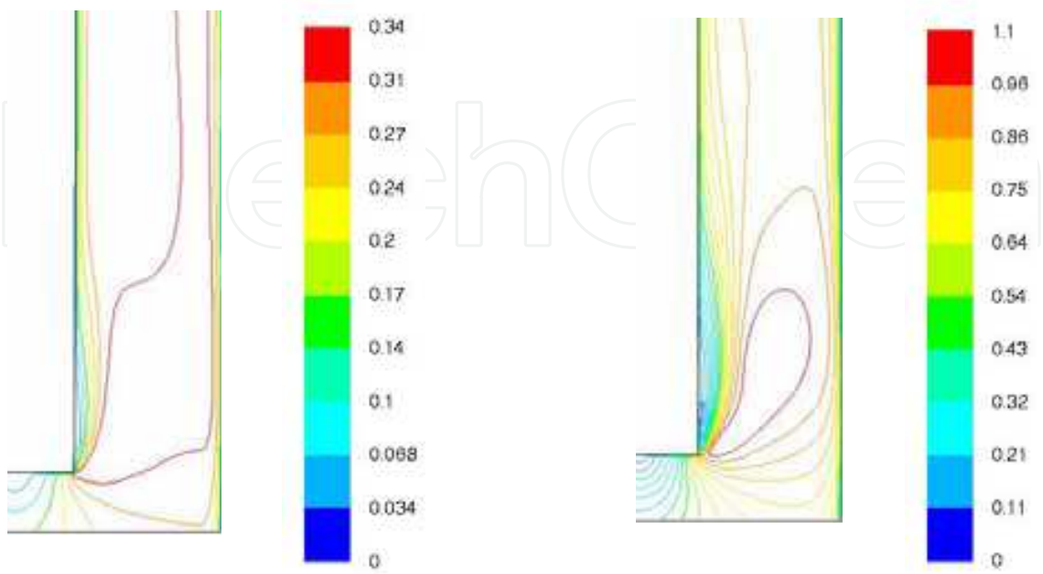

Fig. 14. Computed velocity field (m/s) for water at room temperature flowing in the neighborhood of the flat-end cylindrical probe at two free-stream velocities: a) 0.2 m/s and b) 0.6 m/s. Note that the scales are different.

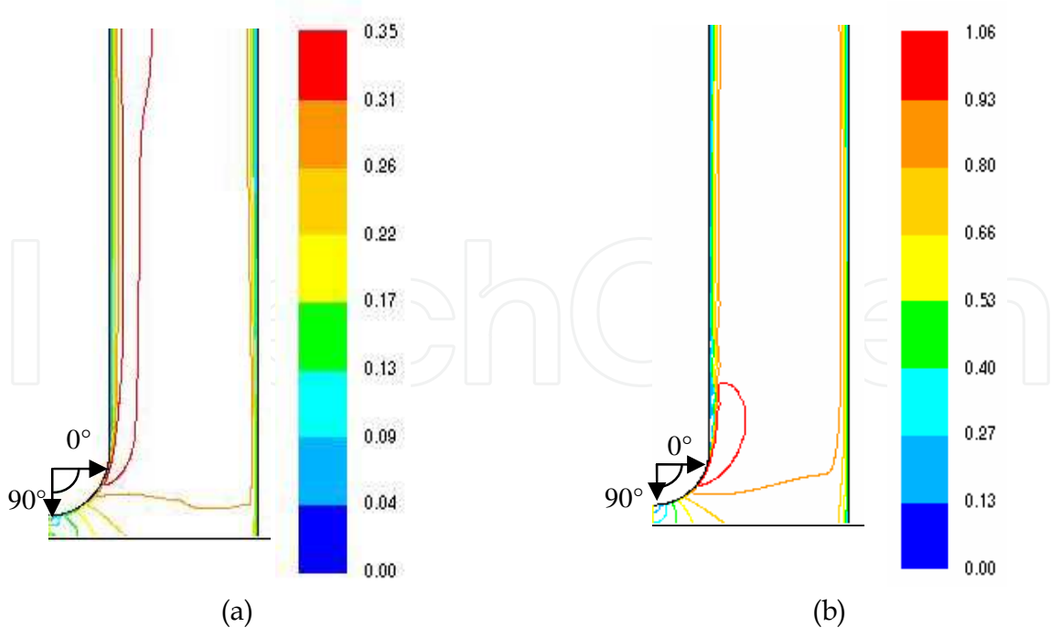

Fig. 15. Computed velocity field (m/s) for water at room temperature flowing in the neighborhood of the hemispherical-end cylindrical probe at two free-stream velocities: a) 0.2 m/s and b) 0.6 m/s. Note that the scales are different.

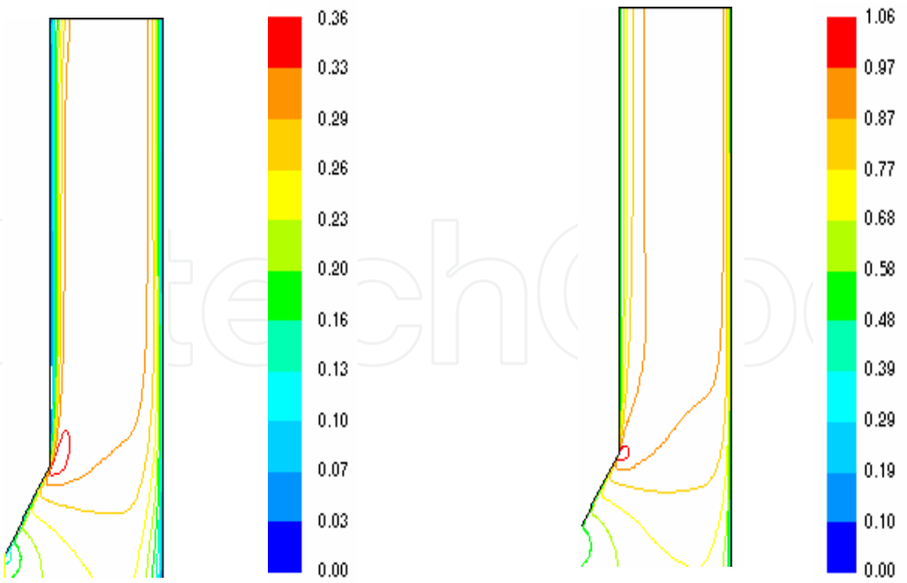

(a) (b)

Fig. 16. Computed velocity field (m/s) for water at room temperature flowing in the neighborhood of the conical-end cylindrical probe at two free-stream velocities: a) 0.2 m/s and b) 0.6 m/s. Note that the scales are different.

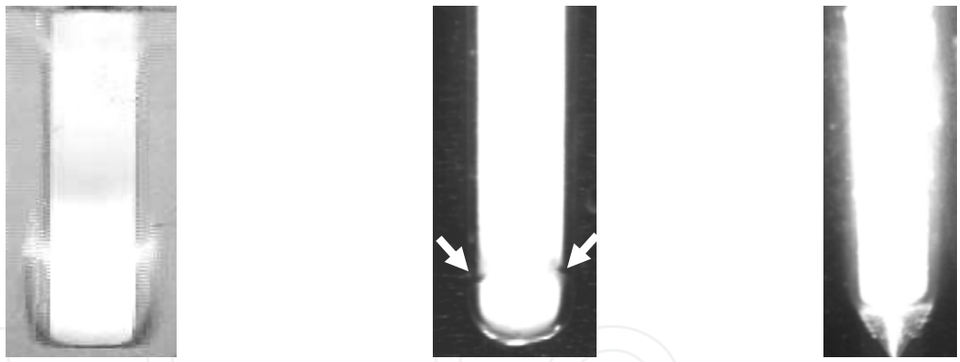

(a) (b) (c)

Fig. 17. Images extracted from the videos during quenching in water at 60°C, flowing at 0.6 m/s, for: a) flat-end cylindrical probe; b) hemispherical-end cylindrical probe and c) conical-end cylindrical probe.

4.3 Wetting front kinematics and heat extraction

In the previous section it was established that the conical-end cylindrical probe is the best alternative for conducting quenching experiments to characterize wetting front kinematics and obtain heat extraction data. Thus, in this subsection results obtained with this probe geometry are presented.

For a given quench medium, the heat extraction is influenced by the quench bath temperature and the degree of agitation. The latter has been characterized in the literature in a qualitative as well as in a quantitative fashion; in the former case, terms such as

"moderate", "strong", etc., have been used while in the latter, the quench medium velocity in a specially designed apparatus is used (Totten *et al*., 1993). In the following, the effect of the water velocity on wetting front kinematics and heat extraction (using the conical-end cylindrical probe) is presented.

The temperature response at the position of T/C 1 in Figure 18 (a) and the corresponding cooling rate history for quenching in water at 60 °C, flowing at several velocities are plotted in Figure 18 (b). Regarding the thermal response, the curves shift to the left as the water velocity increases which implies that the total quenching time is reduced; also, the duration of the film boiling stage (the part of the curve where the temperature decreases at a constant rate) decreases as the water velocity increases. The cooling rate history curves show increasing maximum values as the water velocity increases. For the conical-end cylindrical probe, the re-wetting time is directly related to heat transfer in the neighbourhood of the probe tip, which acts as a heat sink. Thus, increasing water velocity favours an increase in the rate at which the probe tip cools, resulting in a lower re-wetting time (the time required to break down the vapor blanket) and, therefore, the probe is hotter at a given longitudinal position which, combined with the higher heat extraction capability of water flowing at a higher velocity, results in the behavior observed in Figure 18 (b).

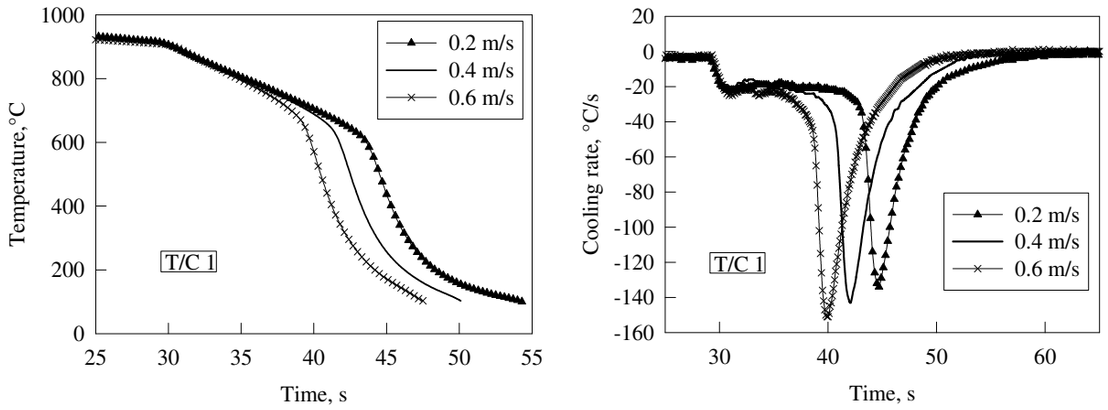

(a) (b)

Fig. 18. a) Thermal response and b) corresponding cooling rate history, as a function of water velocity, during quenching with water at 60 °C.

The wetting front is defined as the *loci* of the boundary between the vapor film blanket and the nucleate boiling zone. Therefore, the wetting front velocity may be estimated by recording the times at which the wetting front passes at previously determined locations along the probe surface; this information was obtained from the video-recordings. As an example, Figure 19 shows a plot of the wetting front position as a function of time for a quench in water at 60 °C, flowing at 0.2 m/s. It is evident that the points follow a straight line which implies a constant wetting front velocity; therefore, a linear regression was applied and is also shown in the figure. The slope of the linear regression was 4.4 mm/s, which is the estimated value of the wetting front velocity in the cylindrical region of the probe for these experimental conditions. The fact that R^2 is very close to 1.0 indicates an excellent agreement between the model and the experimental data.

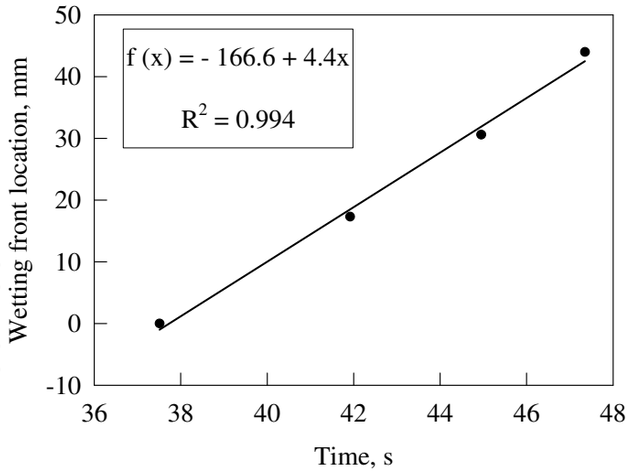

Fig. 19. Wetting front location as a function of quenching time during quenching of a conical-end cylindrical probe with water at 60 °C, flowing at 0.2 m/s. The line represents the estimated values assuming a linear regression.

This procedure was applied along with the video-recordings taken during experiments with water at 60 °C, flowing at 0.4 and 0.6 m/s. The results, expressed as wetting front velocity as a function of water velocity, are plotted in Figure 21. The wetting front velocity increases in a non-linear fashion as the water velocity is increased.

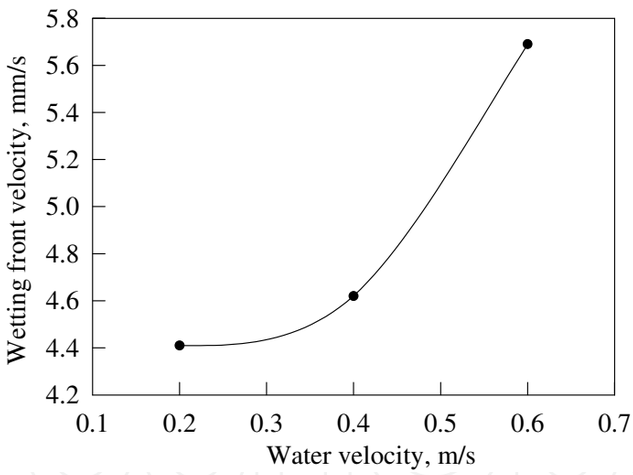

Fig. 20. Wetting front velocity as a function of water velocity for experiments with water at 60 °C.

The heat extraction at the probe/quench medium interface is usually characterized by either a heat transfer coefficient or a surface heat flux; given the several heat extraction modes present during the quench, both of these quantities vary as the quench progresses. Using the thermal responses shown in Figure 20 as input, the surface heat flux was estimated applying the sequential function specification technique (Beck *et al.*, 1982) whose algorithm has been implemented in the in-house code WinProbe (Meekisho *et al.*, 2005). The code considers 1D heat flow, which in the context of these experiments implies ignoring any heat transferred in the axial direction. The resulting surface heat flux histories for the three water velocities studied are plotted in Figure 21 (for thermocouple location T/C 1). As can be seen in the

figure, the surface heat flux remains constant during the vapor blanket stage; later on during each experiment heat extraction increases sharply as the vapor blanket collapses giving way to the nucleate boiling regime until a maximum value (also known in the literature as the critical heat flux – CHF) is reached. The heat flux then decreases as boiling ceases and heat is extracted by convection alone.

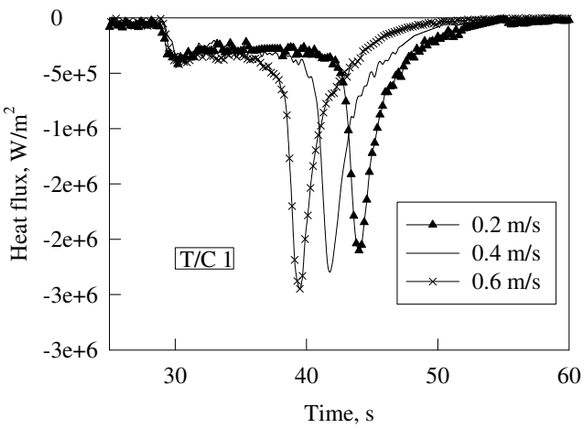

Fig. 21. Surface heat flux history for experiments with water at 60 °C, at the position of T/C 1.

The maximum surface heat flux is plotted, as a function of water velocity, in Figure 22. From these values, a linear regression was applied resulting in a high value of R^2. This is the first step towards building empirical models for the surface heat flux history curves.
In Figure 23, images extracted from the video-recording of quenching of a conical-end cylindrical probe in water at 60 °C, flowing ar 0.2 m/s are shown. The original images were modified with the imaq Vision Builder (National Instruments) software to highlight details of the events at the probe surface. The images clearly show that the two heat transfer modes that combine boiling and forced convection (film boiling and nucleate boiling) may be subdivided. The nucleate boiling area is comprised by two zones: a) one close to the wetting front, where a high density of relatively small bubbles is evident and b) another, where fewer but larger bubbles are formed. Regarding the film boiling area, there is a zone (near the wetting front) where the probe surface is significantly cooler than the rest of the surface covered by the vapor blanket.

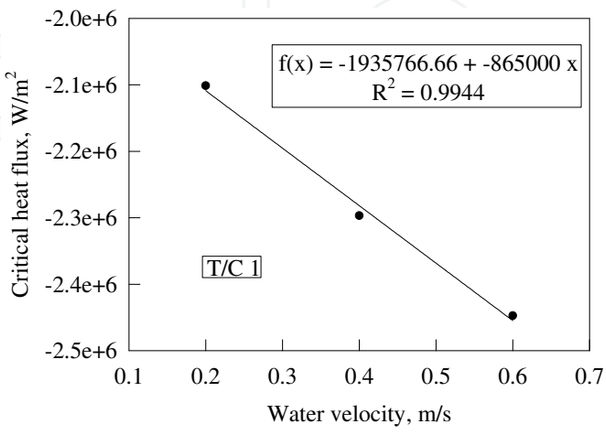

Fig. 22. Critical heat flux as a function of water velocity for experiments with water at 60 °C, at the position of T/C 1.

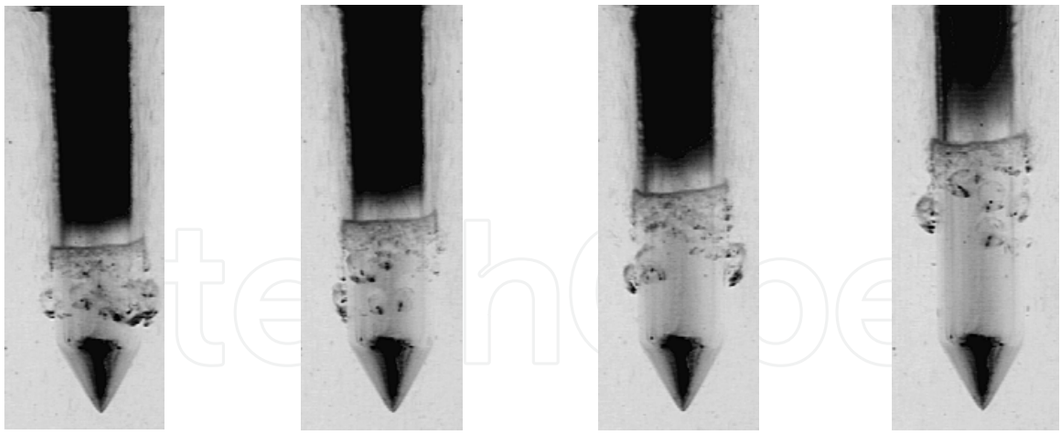

(a) (b) (c) (d)

Fig. 23. Boiling events at the probe surface during a quench from 900 °C with water at 60 °C, flowing at 0.2 m/s; (a) 7.71 s, (b) 8.51 s, (c) 9.31 s, (d) 10.81 s after the start of the quench.

5. Conclusion

Hydrodynamic conditions near the probe surface control the sequence of events that occur during quenching of metallic probes. Through detailed computational and experimental work we have shown that conical-end cylindrical probes should be preferred over flat.end cylindrical ones, which are currently the common practice. Using the suggested probe we were able to form estable and symmetrical wetting fronts even for high water velocities which has made possible to establish the effect of water velocity on heat extraction and to distinguish two subzones in the nucleate boiling area.

6. Acknowledgement

We acknowledge Dr. Kyozo Arimoto for his assistance in obtaining and translating the Japanese references discussed herein.

7. References

Beck, J.V.; Litkouhi, B. & St. Clair Jr., C.R. (1982). Efficient sequential solution of the nonlinear inverse heat conduction problem. *Numerical Heat Transfer,* Vol. 5, pp. 275–286

Ben David, M.; Zvirin, Y. & Zimmels, Y. (1999). Determination of the quench velocity and rewetting temperature of hot surfaces: Formulation of a nonisothermal microscale hydrodynamic model. *Physical Review E*, Vol. 59, No. 6, pp. 6687-6698

Benedicks, C. (1908). Experimental Researches on the Cooling Power of Liquids, on Quenching Velocities, and on the Constituents Troostite and Austenite. *J. Iron & Steel Inst*., Vol. 77, pp. 153–257

Canale, L.C.F. & Totten, G.E. (2004). Eliminate Quench Cracking with Uniform Agitation. *Heat Treating Progress*, (july/august 2004), pp. 27-30

Carnahan, B.; Luther, A.H. & Wilkes, J.O. (1969). *Applied Numerical Methods*, John Wiley & Sons, New York, NY, USA

Duffly, R. B. & Porthouse, D. T. C. (1973). The Physics of Rewetting in Water Reactor Engineering Core Cooling. *Nuclear Engineering and Design*, Vol. 31, pp. 234-245

FLUENT. http://www.ansys.com (retrieved January 20, 2011)

Fourier, J. (1820). Mémoire d'Analyse sur le Mouvement de la Chaleur dans les Fluides. *Mem. Acad. Sci. Inst. Fr.*, Vol. 12, pp. 507–530

French, H.J. (1930). *The Quenching of Steels*, The American Society for Steel Treating, Cleveland, OH, USA

Frerichs, F. & Luebben, Th. (2009). The Influence of Surface Temperature on Rewetting Behavior During Immersion Quenching of Hollow and Solid Cylinders. *Journal of ASTM International*, Vol. 6, No. 1, Paper ID JAI101852

Hein, D. (1980) *Modellvorstellung zur Wiederbenetzung durch Fluten*, Ph. D. Thesis, Technical University of Hannover, 182 pp.

Hernández-Morales, B.; López-Valdéz, A.; Vergara-Hernández, H.J.; Sánchez–Sarmiento, G.; Gastón, A. & Totten, G. E. (2009). Experimental Determination of the Temperature Evolution Within the Quenchant During Immersion Quenching, *Proceedings of New Challenges in Heat Treating and Surface Engineering – Conference in Honor of Božidar Ličić*, pp. 31-36, Zagreb, Croatia, June 9-12, 2009

Hernández-Morales, B.; Vergara-Hernández, H.J. & Solorio-Díaz, G. (2011). Fluid dynamics during forced convective quenching of flat-end cylindrical probes, *Proceedings of the WSEAS International Conference on Heat and Mass Transfer (HMT 11)*, pp. 135-141, Puerto Morelos, México, January 29-31, 2011

Jagannath, V. & Prabhu, K. N. (2009). Quench Severity and Kinetics of Wetting of Vegetable Oil Blends and Nanofluids for Heat Treatment, *Proceedings of New Challenges in Heat Treating and Surface Engineering – Conference in Honor of Božidar Ličić*, pp. 17-22, Zagreb, Croatia, June 9-12, 2009

King, L.V. (1914). On the Convection of Heat from Small Cylinders in a Stream of Fluid: Determination of the Convection Constants of Small Platinum Wires with Applications to Hot-Wire Anemometry. *Philos. Trans. R. Soc. London*, Ser. A, 1914, Vol. 214, pp. 373–432

Kobasko, N. I. & Timchenko, N. P. (1986). Cinematographic Investigation of the Cooling process of Alloys in aqueous Polymeric Solution. *Metal Science and Heat Treatment*, Vol. 28, No. 10, pp. 729-734

Kunzel, T. (1986). *Einfluss der Wiederbenetzung auf die allotrope Modifikationsanderung tauchgekiihlter Metallkorper*. Dissertation, Faculty for Mechanical Engineering of the Technical University of Munich, 1986, 138 pp.

Ladish, R. (1980). "Untersuchung der minimalen Filmsiedetemperaturen auf keramischen und metallischen Leitem", Report of "Kemforschungsstelle Karlsruhe", Report No. KfK-2970, 96 pp.

Lainer, K. & Tensi, H.M. (1996). Heat Transfer Coefficient and Heat Flux Density Distribution Influenced by the Wetting Behavior of Hollow Cylinders, *Proceedings of the Second International Conference on Quenching and the Control of Distortion*, pp. 93-100, Cleveland, OH, USA, November 4-7, 1996

Launder, B. E. & Spalding, D. B. (1974). The numerical computation of turbulent flows. *Comput. Methods Appl. Mech. Eng.*, Vol. 3, pp. 269-289

Leidenfrost, G. J. (1966). De Aqua Communis Nonnullis Tractus. Original from 1756. In: C. Waves, *International Journal of MassTransfer*, Vol. 9, pp. 1153-1166 (trans.)

Liscic, B.; Tensi, H.M.; Totten, G.E. & Webster, G.M. (2003). Non-Lubricating Process Fluids: Steel Quenching Technology. In: *Fuels and Lubricants Handbook: Technology, Properties, Performance and Testing* , G.E. Totten, S.R. Westbrook, R.J. Shah (Eds.) , pp. 587-634, ASTM International, West Conshocken, PA.

Loshkaroev, V.E.; Tensi, H.M.; Gese, H. & Stich, A. (1994). Calculation of Temperature and Heat Flux in Quenched Cylinders for Different Wetting Processes. *Steel Research*, Vol. 65, No. 9, pp. 390-395

Lübben, Th.; Frerichs, F.; Hoffmann, F. & Zoch, H.-W. (2009). Rewetting Behavior During Immersion Quenching, *Proceedings of New Challenges in Heat Treating and Surface Engineering – Conference in Honor of Božidar Ličić*, pp. 23-30, Zagreb, Croatia, June 9-12, 2009

Meekisho, L.; Hernández-Morales, B.; Téllez-Martínez, J.S. & Chen, X. (2005). Computer-aided cooling curve analysis using WinProbe. *Int. Journal of Materials and Product Technology*, Vol 24, Nos. 1-4, pp. 155–169

Narazaki, M.; Asada, S. & Fukuhara, K. (1996). Recent Research on Cooling Power of Liquid Quenchants in Japan, *Proceedings of the Second International Conference on Quenching and the Control of Distortion*, pp. 37-46, Cleveland, OH, USA, November 4-7, 1996

Narazaki, M.; Kogawara, M.; Shirayori, A. & Fuchizawa, S. (1999). Influence of Wetting Behaviour on Cooling Characteristics during Quenching of Hot Metal, *Proc. of The 3rd International Conference on Quenching and Control of Distortion*, pp. 112-120, Prague, Czech Republic, March 24-26, 1999

Pilling, N.B. & Lynch, T.D. (1920). Cooling Properties of Technical Quenching Liquids. *Trans. AIME*, Vol. 62, pp. 665–688

Russell, A.S. (1910). The convection of heat from a body cooled by a stream of fluid. *Philos. Mag.*, Vol. 20, No. 118, pp. 591–610

Russell, T.F. (1939). "Some Tests on Quenching Oils", Spec. Report No.24, "Second Report of the Alloy Steels Research Committee," Iron and Steel Inst., London, 1939, Section IX, Part 6, pp. 283–298

Sato, S. (1933) On the Effect of Facing on the Cooling Velocity of a specimen during Quenching. *Metal Research* , Vol.10 , No.2 , pp. 63–70 (in Japanese)

Scott , H. (1934). The Problem of Quenching Media for the Hardening of Steel. *Trans. ASM*, Vol. 22, pp. 577–604

Speith, K.G. & Lange, H. (1935). Ueber das Abschreckvermögen flüssiger Härtemittel. *Mitt. Kais. – Wilh. –Inst. Eisenforschg.*, Vol. 17, pp. 175–184

Stich, A.; Spengler, A.; Spies, H.J. & Tensi H.M. (1996). Effect of probe geometry on cinematics and hardness for water quenching. *Harterei-Technische Mitteilungen,* Vol. 51, No. 4, pp. 215–222

Stitzelberger-Jakob, P. (1961). "Hartevorherbestimmung mit Hilfe des Benetzungsablaufes beim Tauchkiihlen von Stahlen", Dissertation, Faculty for Mechanical Engineering of the Technical University Munich, 160 pp.

Tagaya, M. & Tamura, I. (1952). Studies on the Quenching Media (1st Report) – An Analysis of Cooling Process During Quenching. *Mem. Inst. Sci. Ind. Research*, Vol. 9, pp. 85-102.

Tensi, H.; Stitzelberger-Jakob, P. & Kunzel, T. (1988). Cooling Bath Monitoring and Controlling the Kinematics of Wetting to Prevent Hardening Defects, (in German – "Kinematik der Benetzung uberwachen und steuern zum Vermeiden von Hartefehlern"), *Maschinenmarkt*, Vol. 4, No. 15, pp. 70-72, 74, 76

Tensi, H. M. (1991). Wetting Kinematics, In: *Theory and Technology of Quenching: A Handbook*, B. Liscic, H. M. Tensi, and W. Luty (Eds.), Springer- Verlag, Berlin, Germany

Tensi, H. M.; Stich, A. & Totten, G. E. (1995). Fundamentals of Quenching. *Metal Heat Treating*, (Mar/Apr 1995), pp. 20-28

Tensi, H.M. & Totten, G.E. (1996). Development of the Understanding of the Influence of Wetting Behavior on Quenching and the Merits in These Developments by Prof. Imao Tamura. *Proceedings of the Second International Conference on Quenching and the Control of Distortion*, pp. 17-27, Cleveland, OH, USA, November 4-7, 1996

Tensi, H. M. & Lainer, K. (1997). Wiederbenetzung und Warmeilbergang beim Tauchkiihlen in Hochleistungsolen. *Harterei-Technische Mitteilungen*, Vol. 52, pp. 298-303.

Tensi, H.M. & Lainer, K. (2000). Effect of Concave and Convex Surfaces on the Heat Transfer and Stress Development During Quenching in Synthetic High-Performance Hardening Oils. *Proceedings of the 19th Heat Treating Society Conference Proceedings*, pp. 446-452, Cincinatti, OH, USA, November 1-4, 1999

Tkachuk, T. I.; Rudakova, N. Ya.; Sheremeta, B. K. & Al'tschuler, M.A. (1986). Influence of the Component Composition of Quenching Oils on the Cooling Intensity in the Bubble Boiling Period. *Metal Science and Heat Treatment*, Vol. 28, No. 9-10, pp. 755-758

Tkachuk, T. I.; Sheremeta, B. K.; Rudakova, N. Ya. & Orazova, M. R. (1989). New Quenching Media Based on Petroleum Oils. *Chemistry and Technology of Fuels and Oils*, Vol. 25, No. 4, pp. 201-203

Totten, G.E.; Bates, C.E. & Clinton, N.A. (Eds.). (1993). *Handbook of Quenchants and Quenching Technology*, ASM International, Material Park, OH, USA

Totten, G.E. & Tensi, H.M. (2002). Quenching Fundamentals: Using Conductance Data to Characterize Quenchants. *Heat Treating Progress*, (July/August 2002), pp. O1-O4

Vergara-Hernández, H.J. & Hernández-Morales, B. (2009). A Novel Probe Design to Study Wetting Front Kinematics During Forced Convective Quenching. *Experimental Thermal and Fluid Science*, Vol. 33, pp. 797–807

Vergara-Hernández, H.J.; Hernández-Morales, B.; Solorio-Díaz, G. & Gutiérrez-Gnechi, G. (2010). Effect of vorticity and pressure gradients on wetting front kinematics during

forced convective quenching, *Proc. of the 18th Congress IFHTSE*, pp. 5187-5195, Rio de Janeiro, Brazil, July 26-30, 2010

Versteeg, H.K. & Malalasekera, W. (1995). *An Introduction to computational fluid dynamics. The finite volume method*. Wiley, New York, NY, USA

Yamanouchi, A., (1968). Effect of Core Spray Cooling in Transient State after Loss of Cooling Accident. *Journal of Nuclear Science and Technology*, No. 5, pp. 547-558

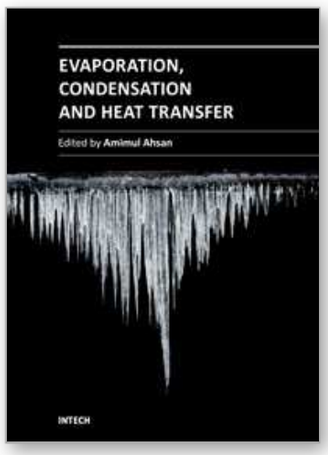

Evaporation, Condensation and Heat transfer
Edited by Dr. Amimul Ahsan

ISBN 978-953-307-583-9
Hard cover, 582 pages
Publisher InTech
Published online 12, September, 2011
Published in print edition September, 2011

The theoretical analysis and modeling of heat and mass transfer rates produced in evaporation and condensation processes are significant issues in a design of wide range of industrial processes and devices. This book includes 25 advanced and revised contributions, and it covers mainly (1) evaporation and boiling, (2) condensation and cooling, (3) heat transfer and exchanger, and (4) fluid and flow. The readers of this book will appreciate the current issues of modeling on evaporation, water vapor condensation, heat transfer and exchanger, and on fluid flow in different aspects. The approaches would be applicable in various industrial purposes as well. The advanced idea and information described here will be fruitful for the readers to find a sustainable solution in an industrialized society.

How to reference
In order to correctly reference this scholarly work, feel free to copy and paste the following:

B. Hernández-Morales, H.J. Vergara-Hernández, G. Solorio-Dĩaz and G.E. Totten (2011). Experimental and Computational Study of Heat Transfer During Quenching of Metallic Probes, Evaporation, Condensation and Heat transfer, Dr. Amimul Ahsan (Ed.), ISBN: 978-953-307-583-9, InTech, Available from: http://www.intechopen.com/books/evaporation-condensation-and-heat-transfer/experimental-and-computational-study-of-heat-transfer-during-quenching-of-metallic-probes

INTECH
open science | open minds

InTech Europe
University Campus STeP Ri
Slavka Krautzeka 83/A
51000 Rijeka, Croatia
Phone: +385 (51) 770 447
Fax: +385 (51) 686 166
www.intechopen.com

InTech China
Unit 405, Office Block, Hotel Equatorial Shanghai
No.65, Yan An Road (West), Shanghai, 200040, China
中国上海市延安西路65号上海国际贵都大饭店办公楼405单元
Phone: +86-21-62489820
Fax: +86-21-62489821

IntechOpen